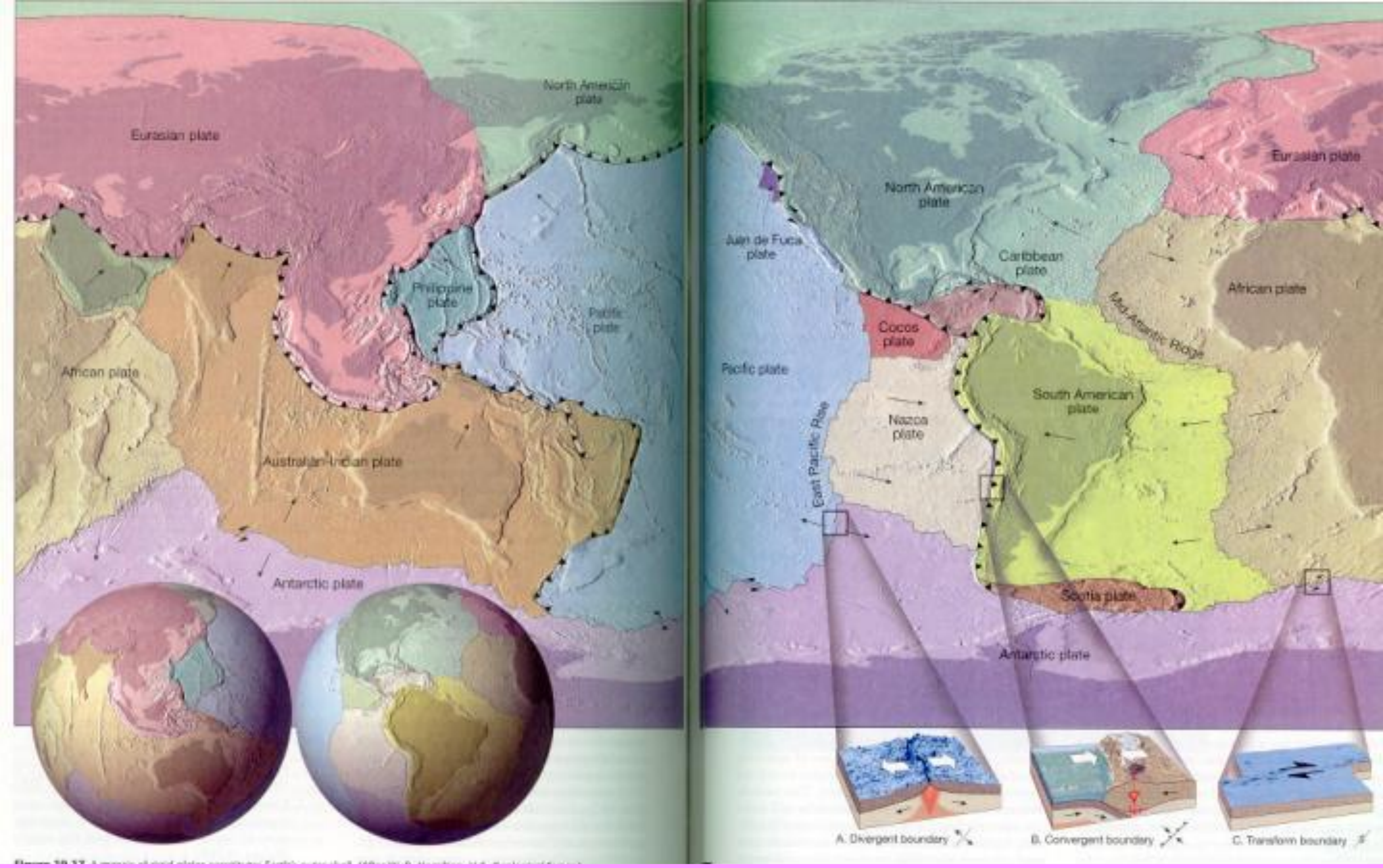

LEVHA TEKTONİĞİ

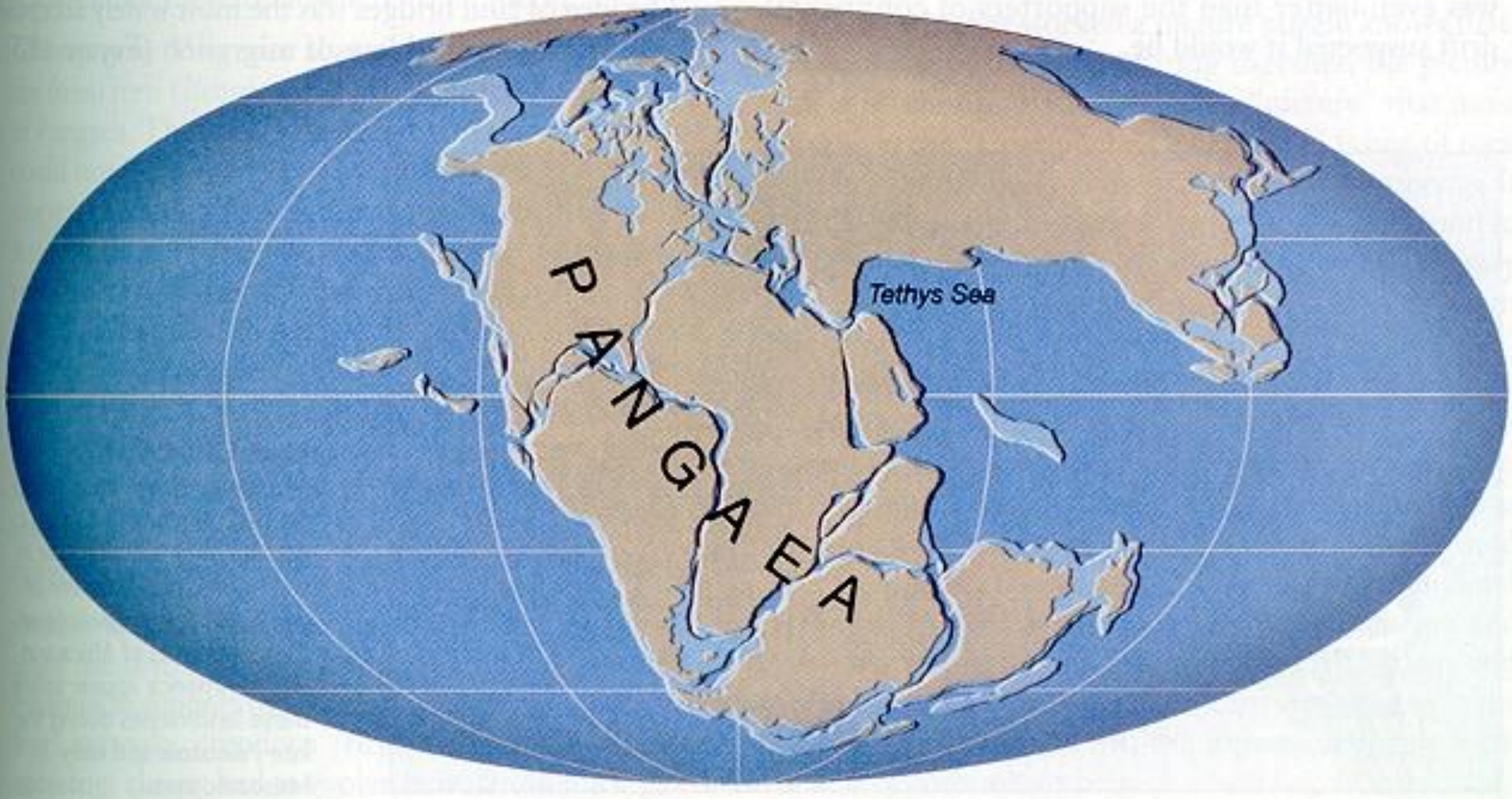

Figure 19.2 Reconstruction of Pangaea as it is thought to have appeared 200 million years ago.

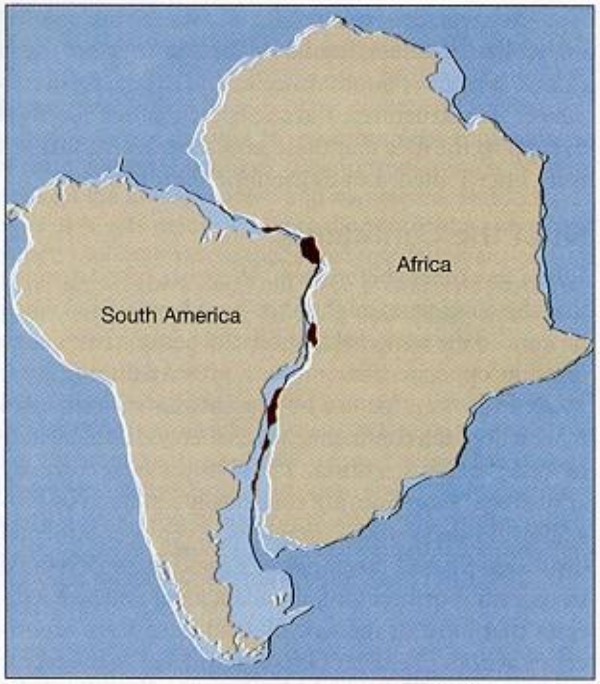

Figure 19.3 This shows the best fit of South America and Africa along the continental slope at a depth of 500 fathoms (about 900 meters). The areas where continental blocks overlap appear in brown. (After A. G. Smith, "Continental Drift." In *Understanding the Earth*, edited by I. G. Gass.

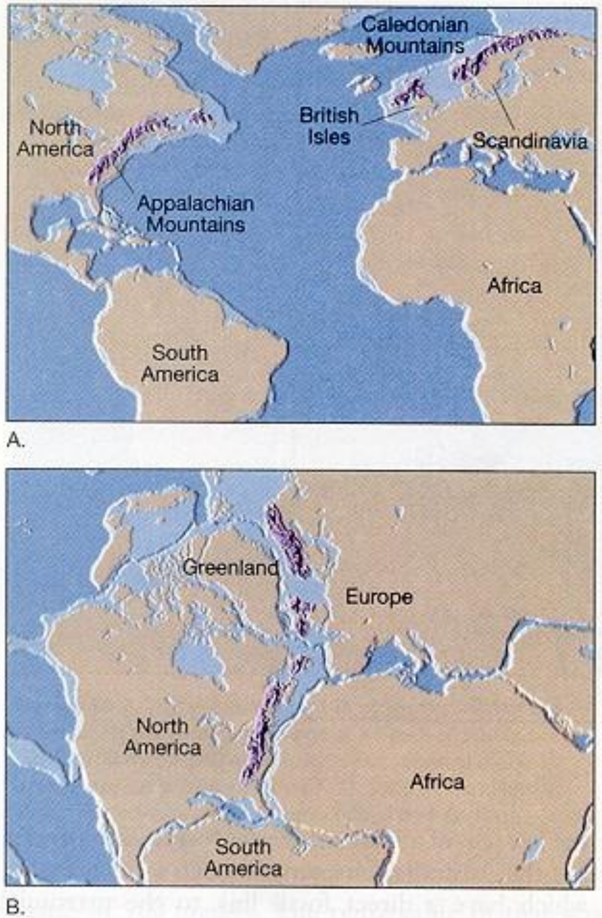

Figure 19.6 Matching mountain ranges across the North Atlantic. A. The Appalachian Mountains trend along the eastern flank of North America and disappear off the coast of Newfoundland. Mountains of comparable age and structure are found in the British Isles and Scandinavia. B. When these landmasses are placed in their predrift locations, these ancient mountain chains form a nearly continuous belt. These folded mountain belts formed roughly 300 million years ago as the landmasses collided during the formation of the supercontinent of Pangaea.

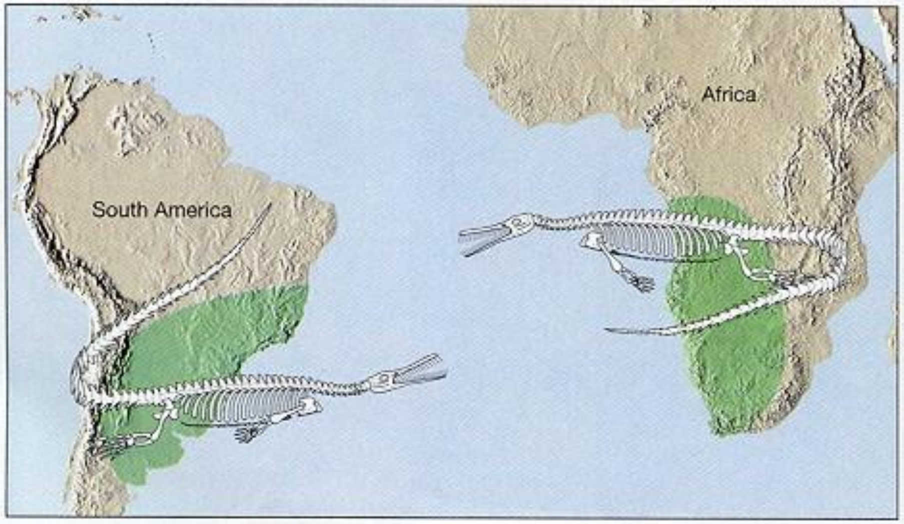

Figure 19.4 Fossils of *Mesosaurus* have been found on both sides of the South Atlantic and nowhere else in the world. Fossil remains of this and other organisms on the continents of Africa and South America appear to link these landmasses during the late Paleozoic and early Mesozoic eras.

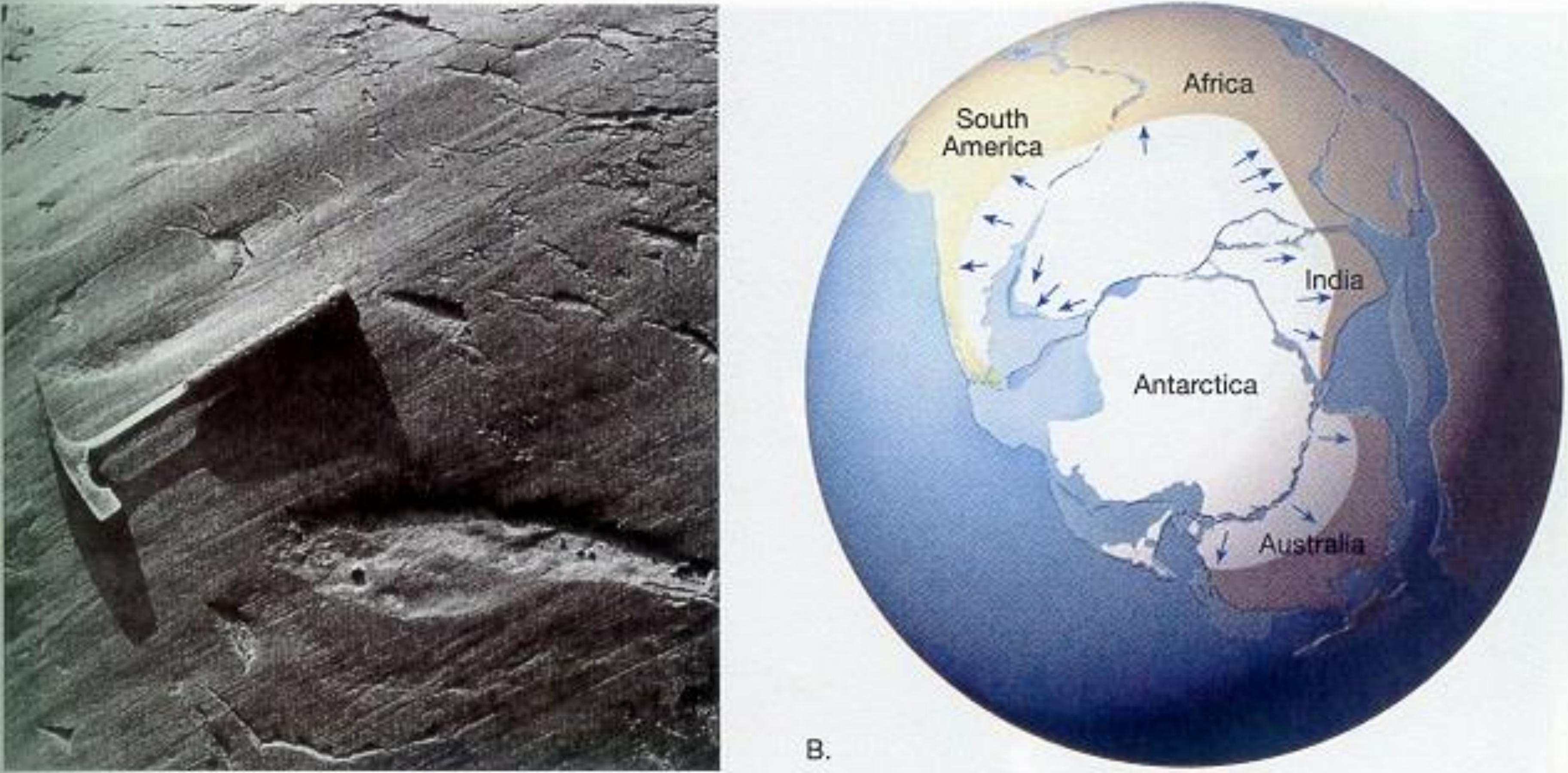

A.

B.

Figure 19.7 A. Glacial striations in the bedrock of Hallet Cove, South Australia, indicate direction of ice movement. (Photo by W. B. Hamilton, U.S. Geological Survey) B. Direction of ice movement in the southern supercontinent called Gondwanaland according to those who developed the continental drift hypothesis.

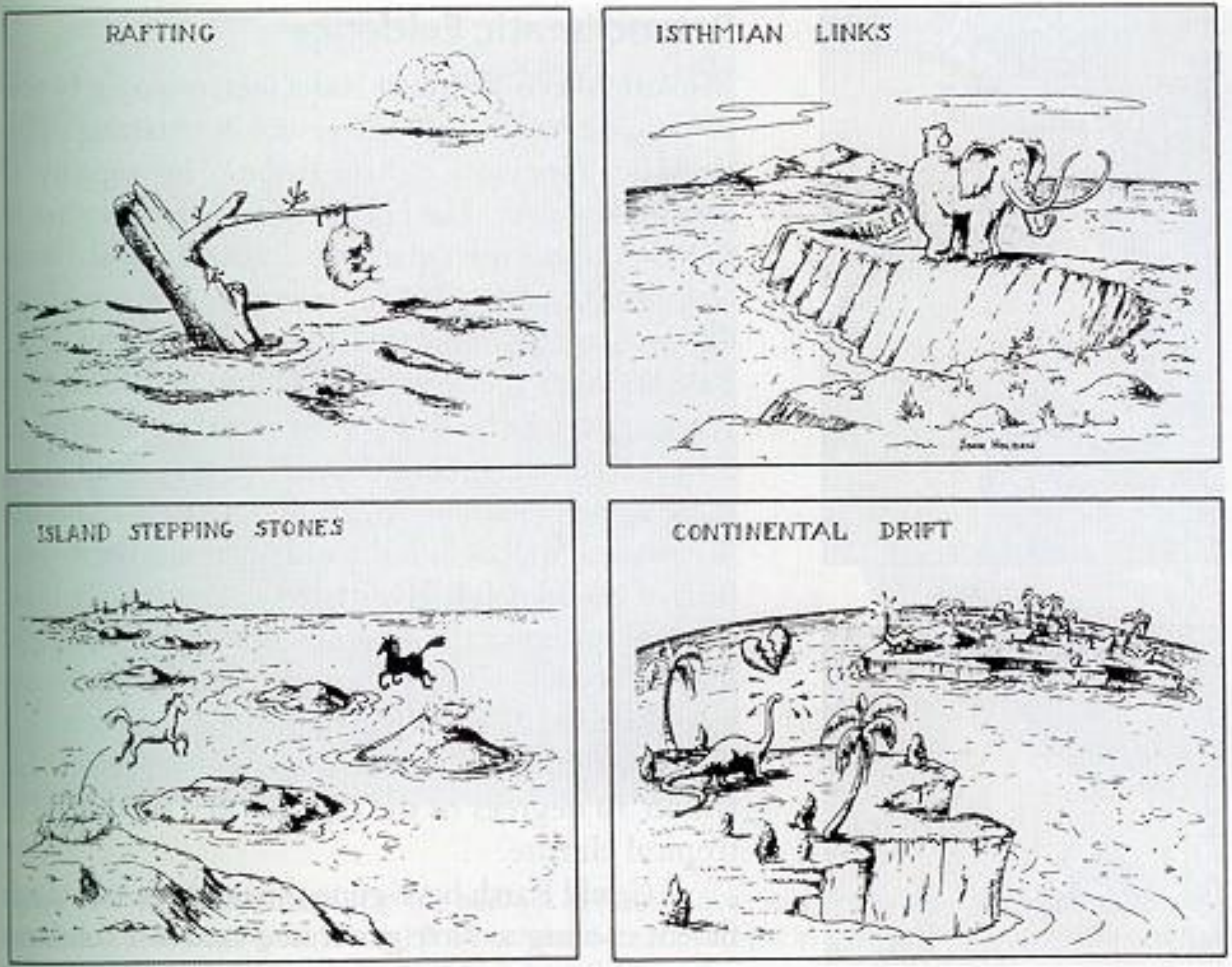

Figure 19.5 These sketches by John Holden illustrate various explanations for the occurrence of similar species on landmasses that are presently separated by vast oceans. (Reprinted with permission of John Holden)

Figure 19.8 Alfred Wegener shown waiting out the 1912–1913 Arctic winter during an expedition to Greenland, where he made a 1200-kilometer traverse across the widest part of the island's ice sheet. (Photo courtesy of Bildarchiv Preussischer Kulturbesitz, Berlin)

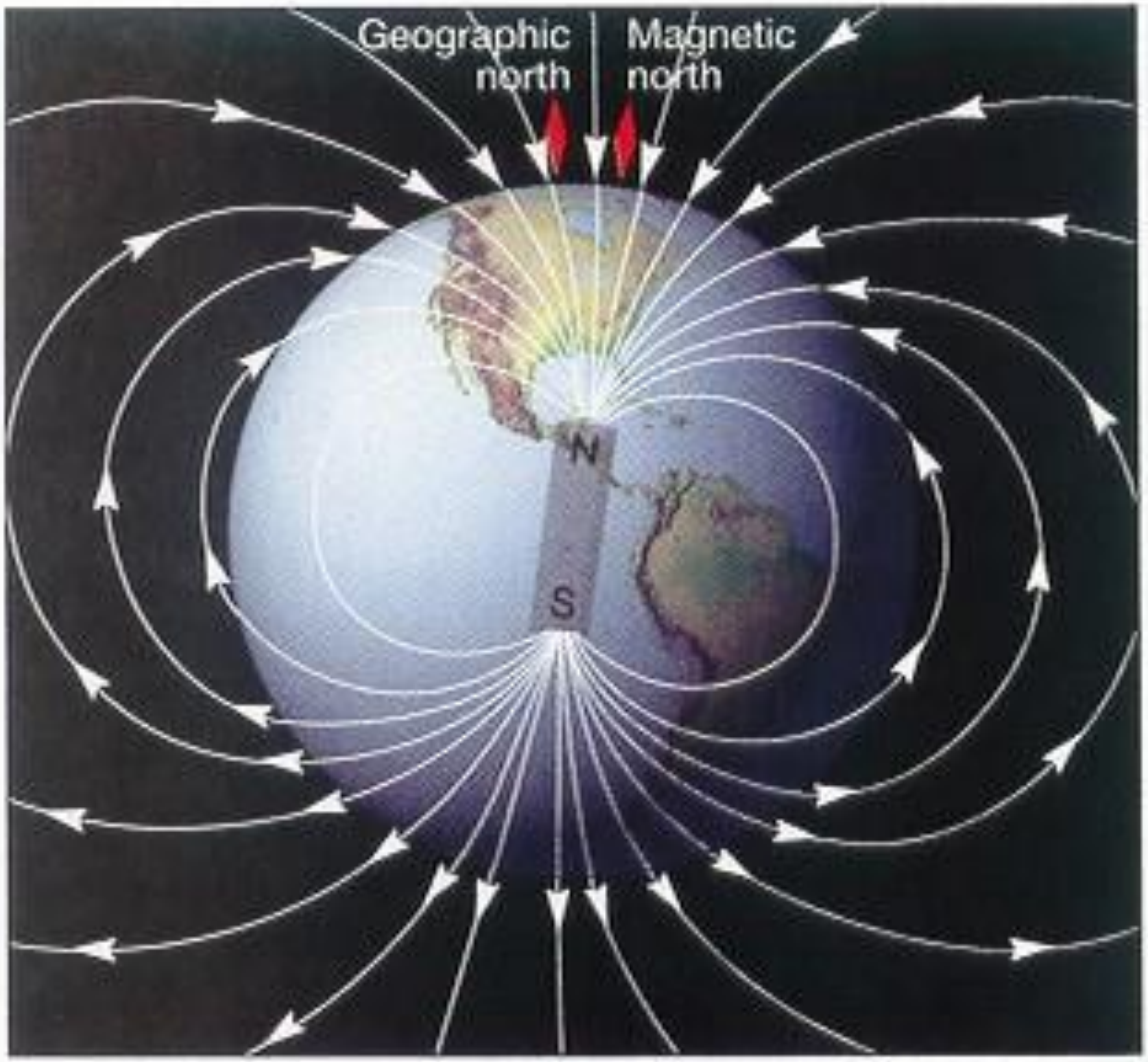

Figure 19.9 Earth's magnetic field consists of lines of force much like those a giant bar magnet would produce if placed at the center of Earth.

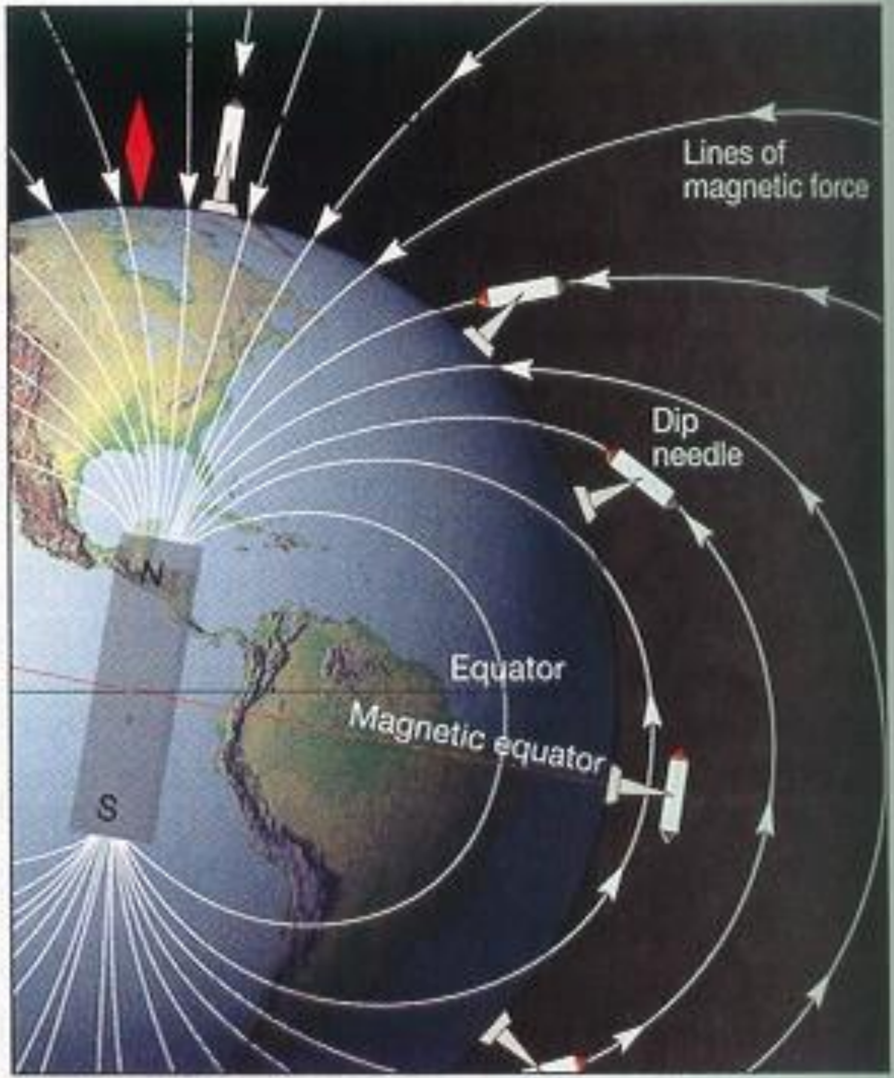

Figure 19.10 Earth's magnetic field causes a dip needle (compass oriented in a vertical plane) to align with the lines of magnetic force. The dip angle decreases uniformly from 90 degrees at the magnetic poles to 0 degrees at the magnetic equator. Consequently, the distance to the magnetic poles can be determined from the dip angle.

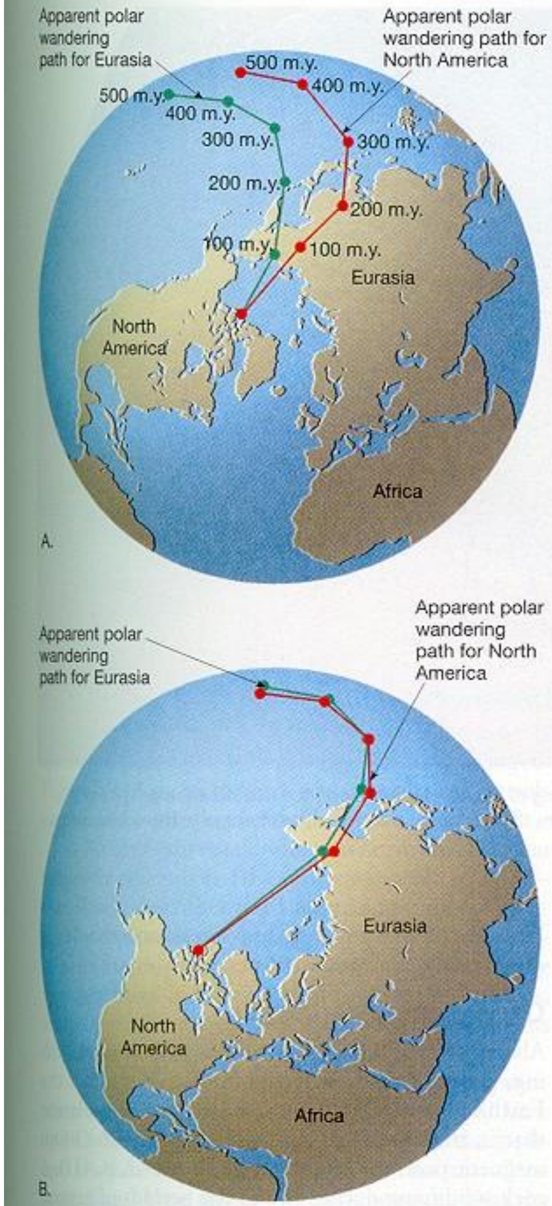

Figure 19.11 Simplified apparent polar-wandering paths as established from North American and Eurasian paleomagnetic data. **A.** The more westerly path determined from North American data was caused by the westward movement of North America by about 24 degrees from Eurasia. **B.** The positions of the wandering paths when the landmasses are reassembled.

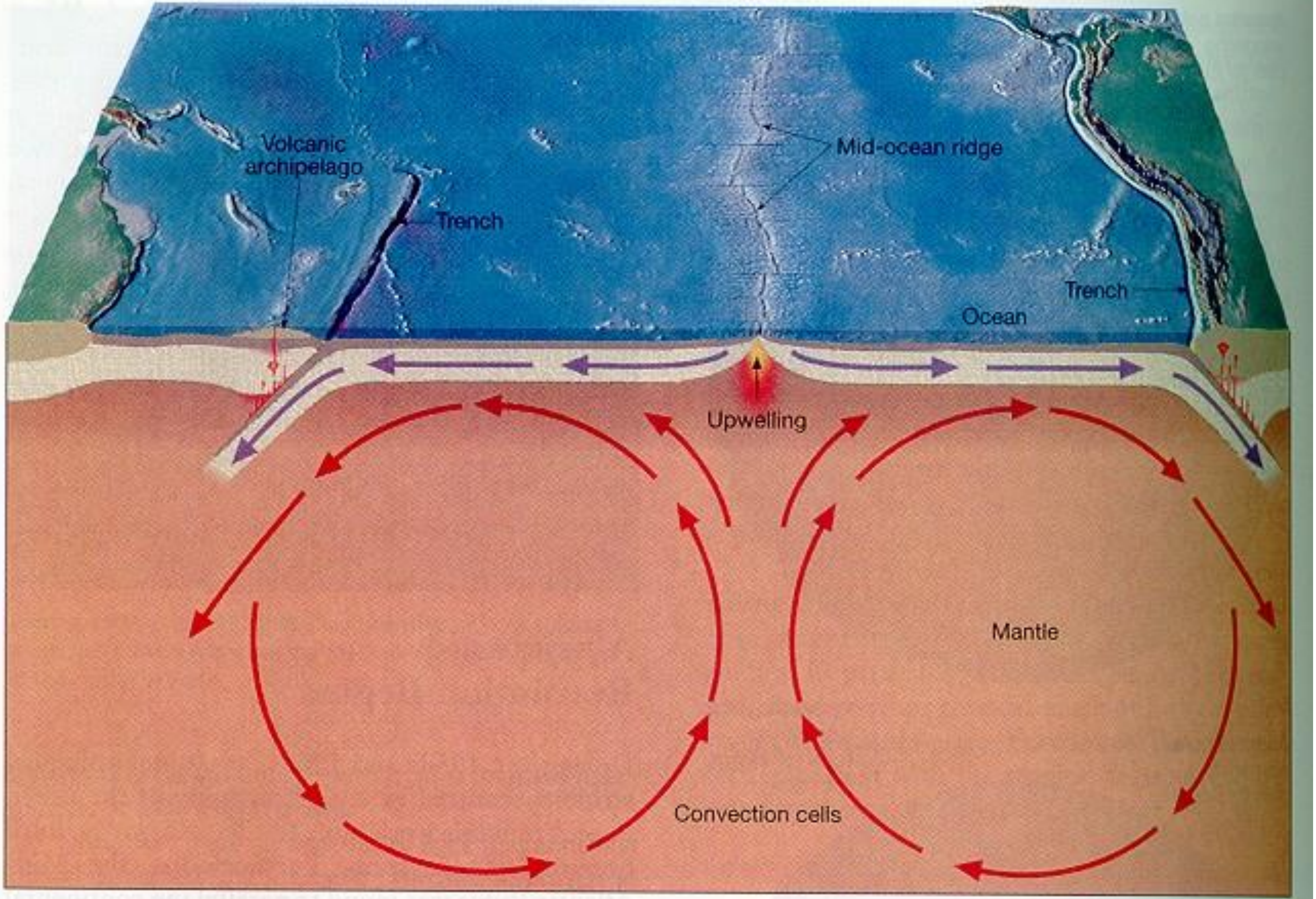

Figure 19.12 Seafloor spreading. Harry Hess proposed that upwelling of mantle material along the mid-ocean ridge system created new seafloor. The convective motion of mantle material carries the seafloor in a conveyor-belt fashion to the deep-ocean trenches, where the seafloor descends into the mantle.

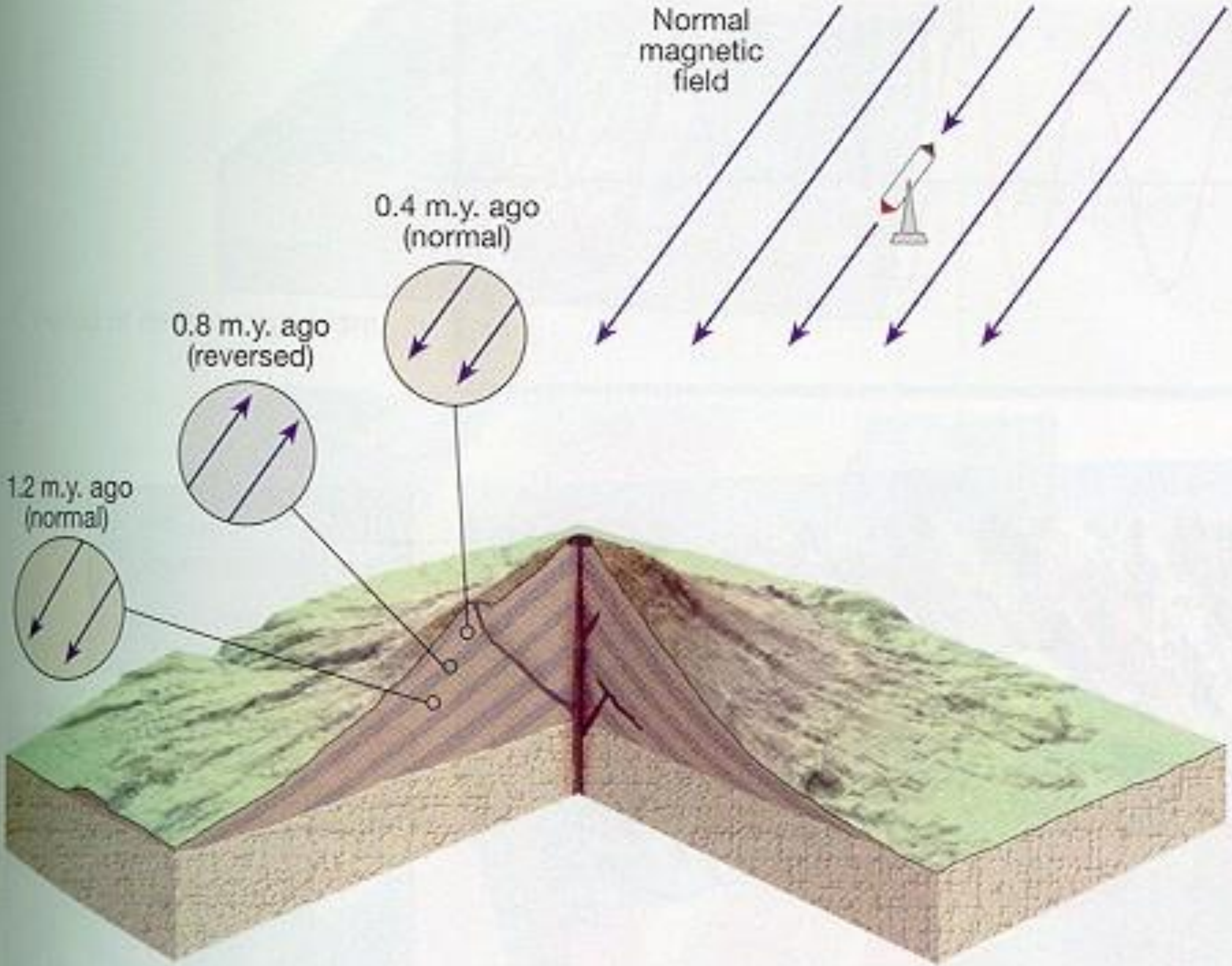

Figure 19.13 Schematic illustration of paleomagnetism preserved in lava flows of various ages. Data such as these from various locales were used to establish the time scale of polarity reversals shown in Figure 19.14.

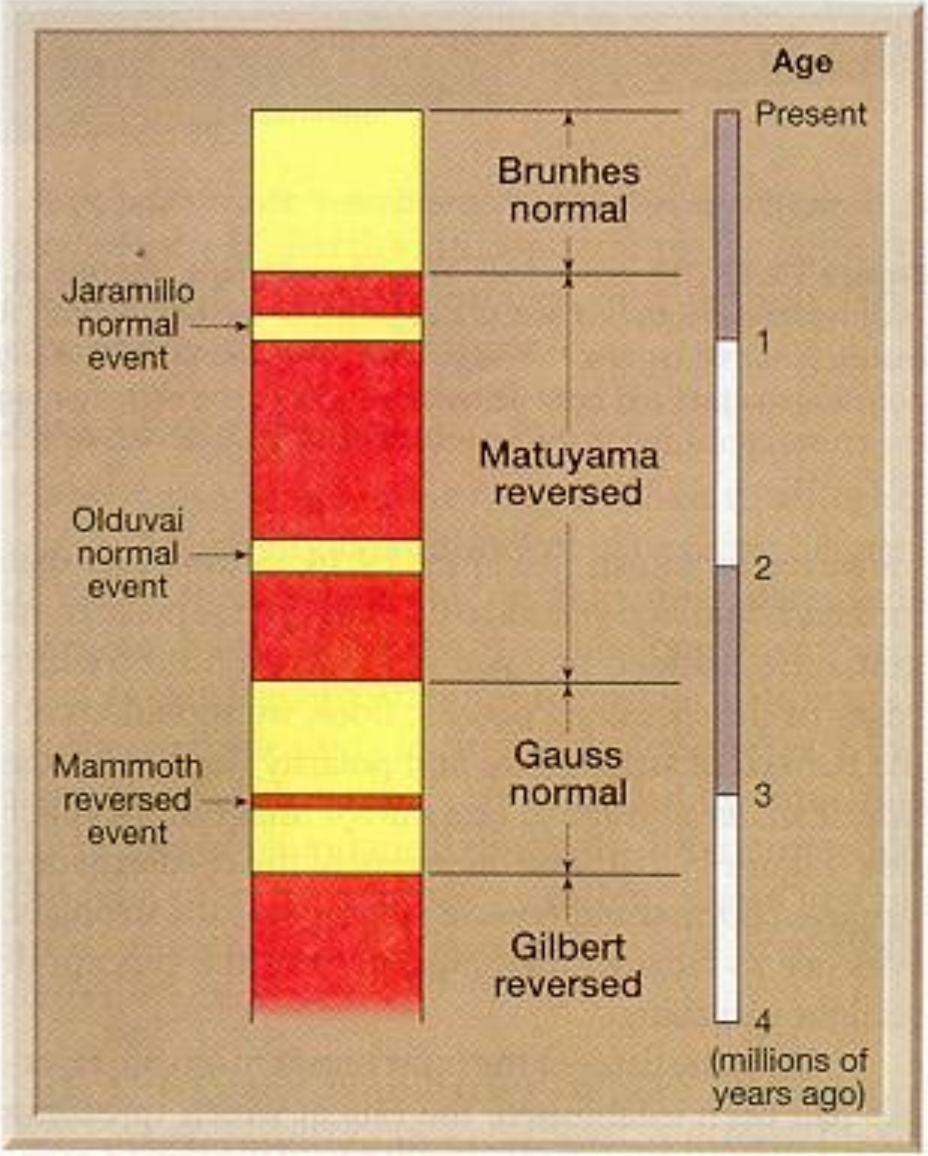

Figure 19.14 Time scale of Earth's magnetic field in the recent past. This time scale was developed by establishing the magnetic polarity for lava flows of known age. (Data from Allen Cox and G. B. Dalrymple)

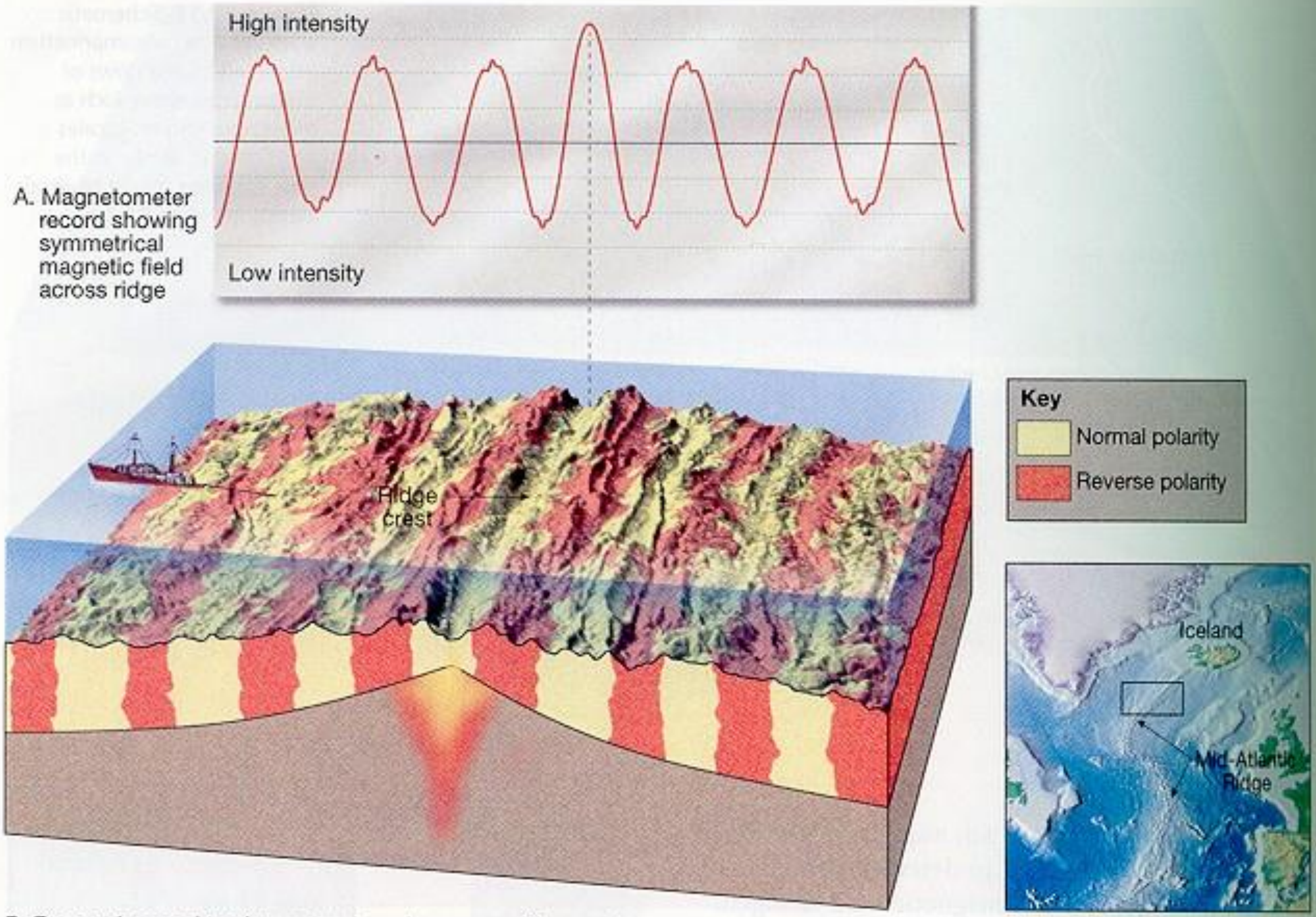

A. Magnetometer record showing symmetrical magnetic field across ridge

B. Research vessel towing magnetometer across ridge crest

C. Location map

Figure 19.15 The ocean floor as a magnetic tape recorder. A. Schematic representation of magnetic intensities recorded as a magnetometer is towed across a segment of the Mid-Atlantic Ridge. B. Notice the symmetrical stripes of low- and high-intensity magnetism that parallel the ridge crest. Vine and Matthews suggested that the stripes of high-intensity magnetism occur where normally magnetized oceanic basalts enhance the existing magnetic field. Conversely, the low-intensity stripes are regions where the crust is polarized in the reverse direction, which weakens the existing magnetic field.

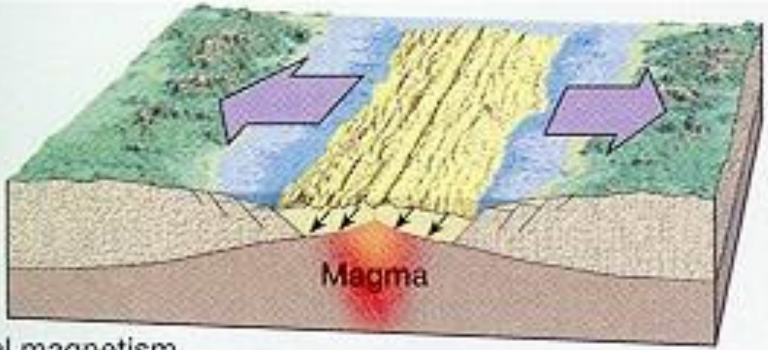

A. Period of normal magnetism

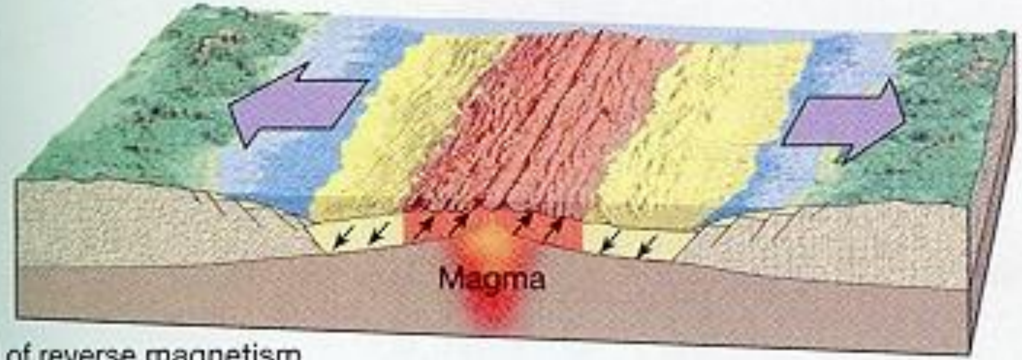

B. Period of reverse magnetism

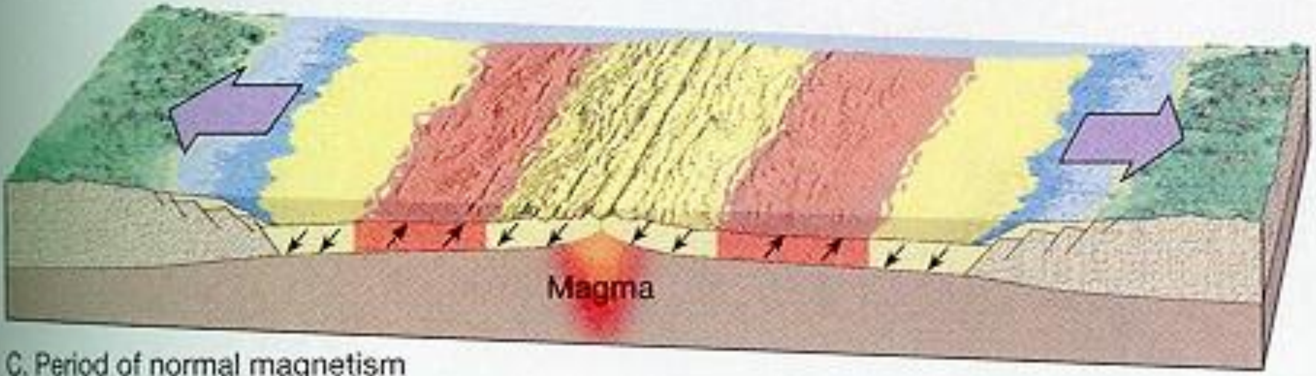

C. Period of normal magnetism

Figure 19.16 As new basalt is added to the ocean floor at mid-ocean ridges, it is magnetized according to Earth's existing magnetic field. Hence, it behaves much like a tape recorder as it records each reversal of the planet's magnetic field.

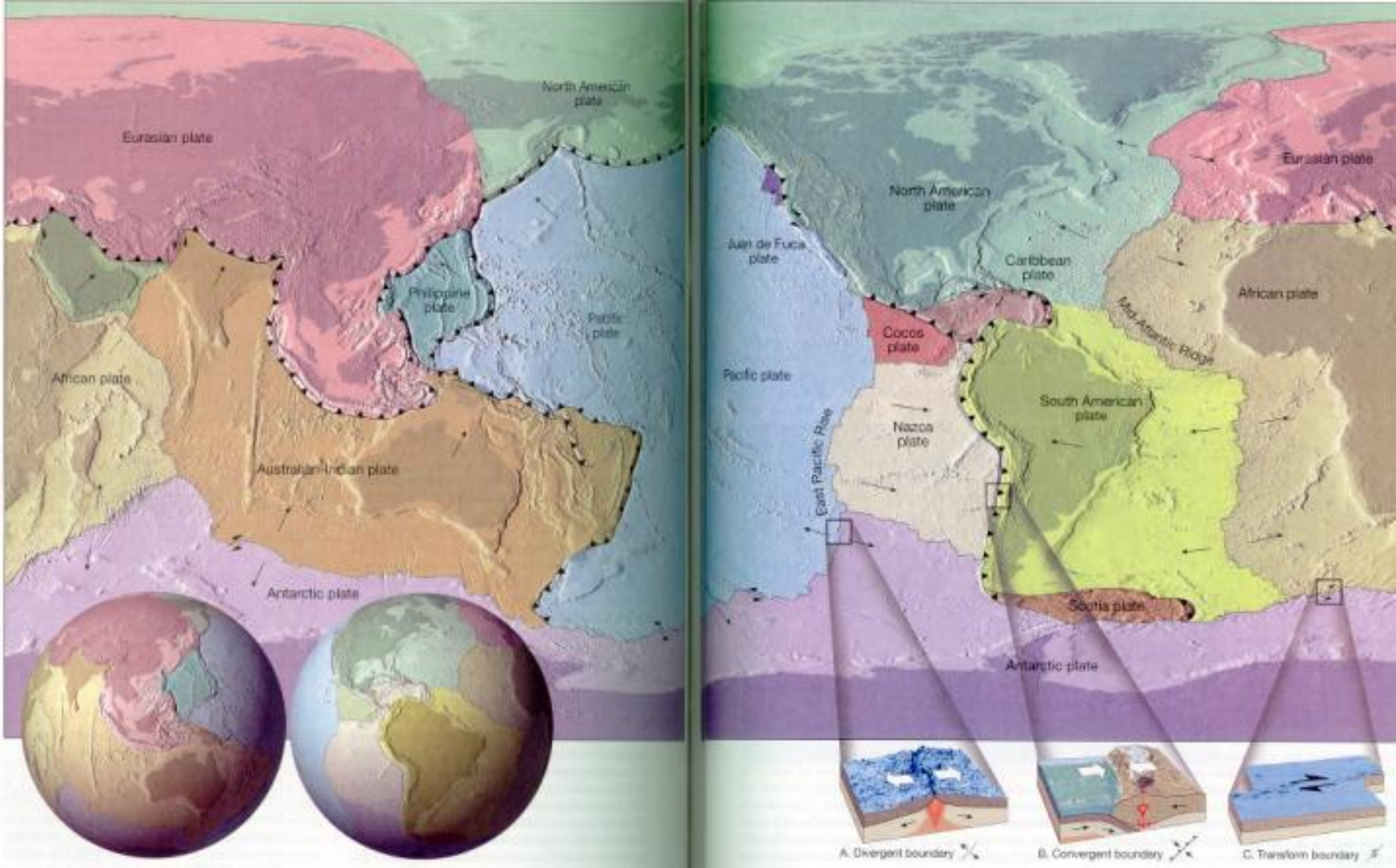

A. Divergent boundary

B. Convergent boundary

C. Transform boundary

Figure 19.17 A mosaic of rigid plates constitutes Earth's outer shell. (After W. B. Hamilton, U.S. Geological Survey)

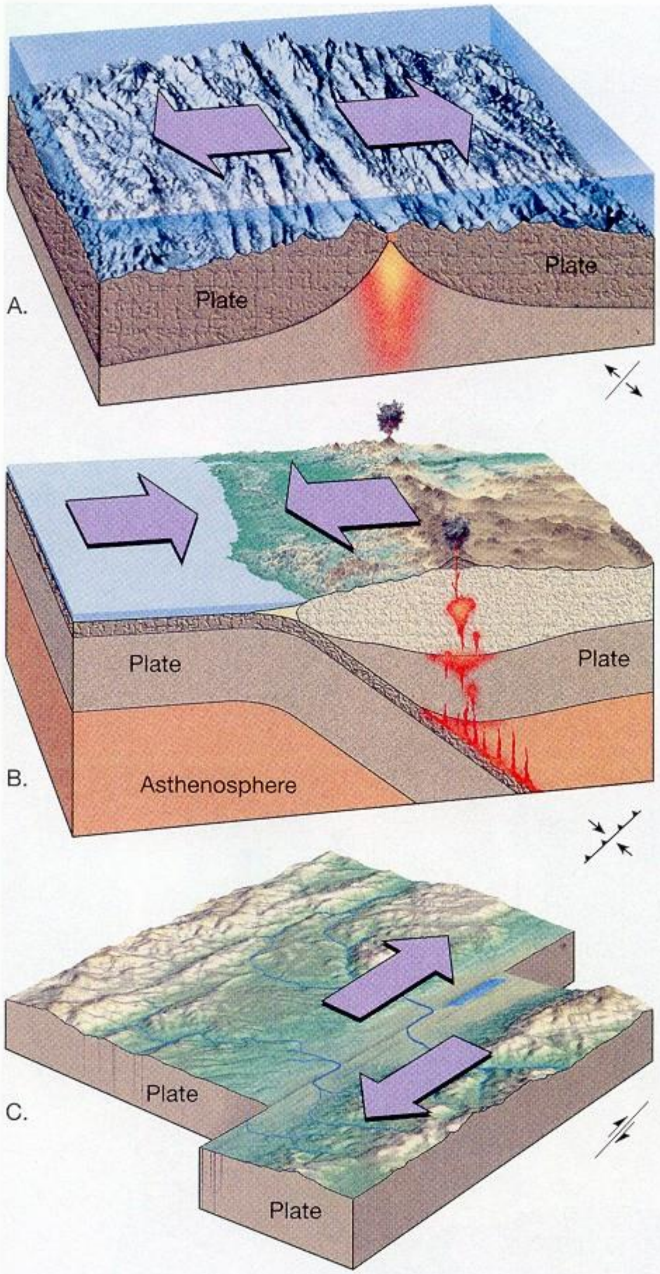

Figure 19.18 Schematic representation of plate boundaries showing the relative motion of plates. **A.** Divergent boundary. **B.** Convergent boundary. **C.** Transform fault boundary.

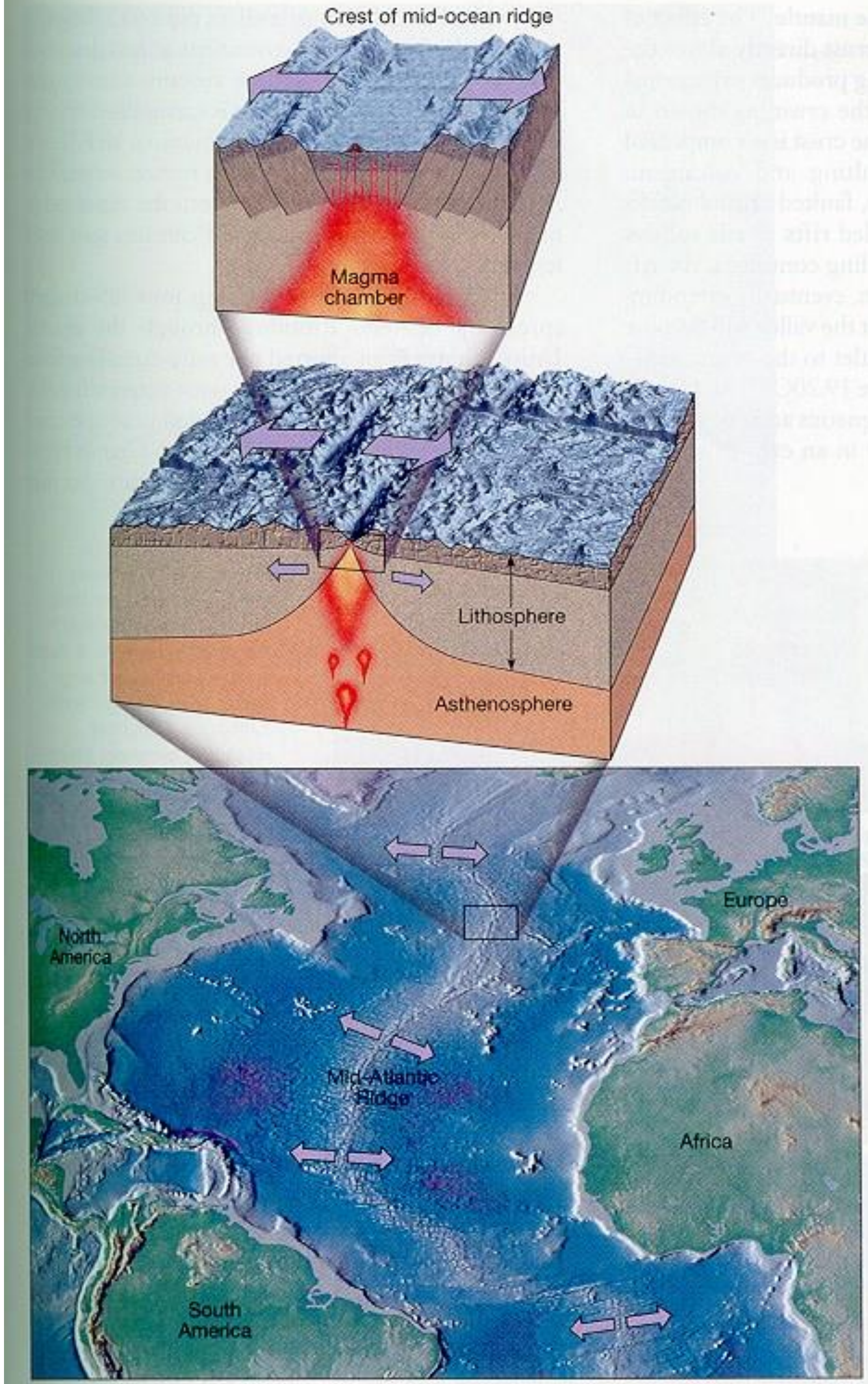

Figure 19.19 Most divergent plate boundaries are situated along the crests of oceanic ridges.

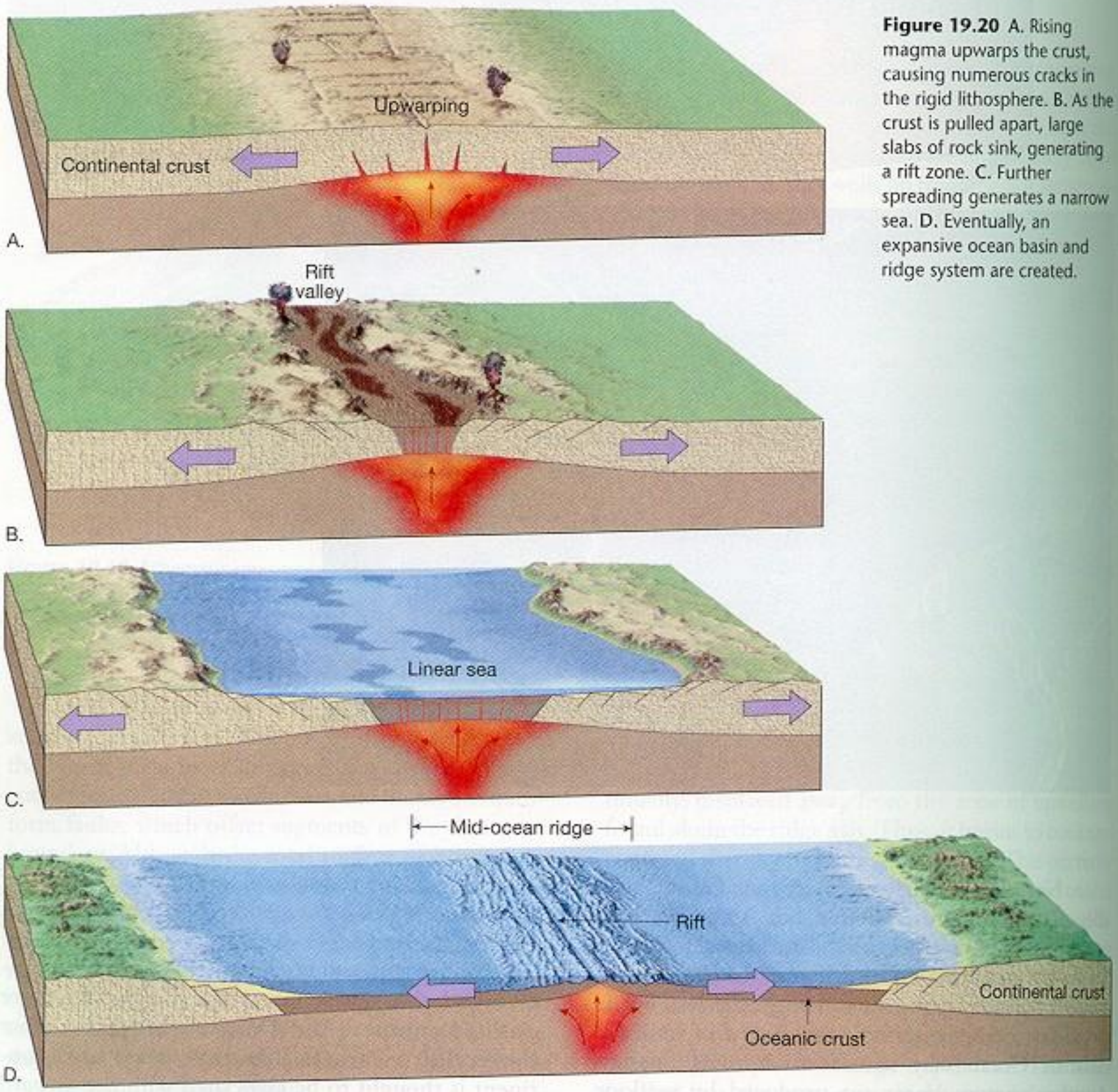

Figure 19.20 **A.** Rising magma upwarps the crust, causing numerous cracks in the rigid lithosphere. **B.** As the crust is pulled apart, large slabs of rock sink, generating a rift zone. **C.** Further spreading generates a narrow sea. **D.** Eventually, an expansive ocean basin and ridge system are created.

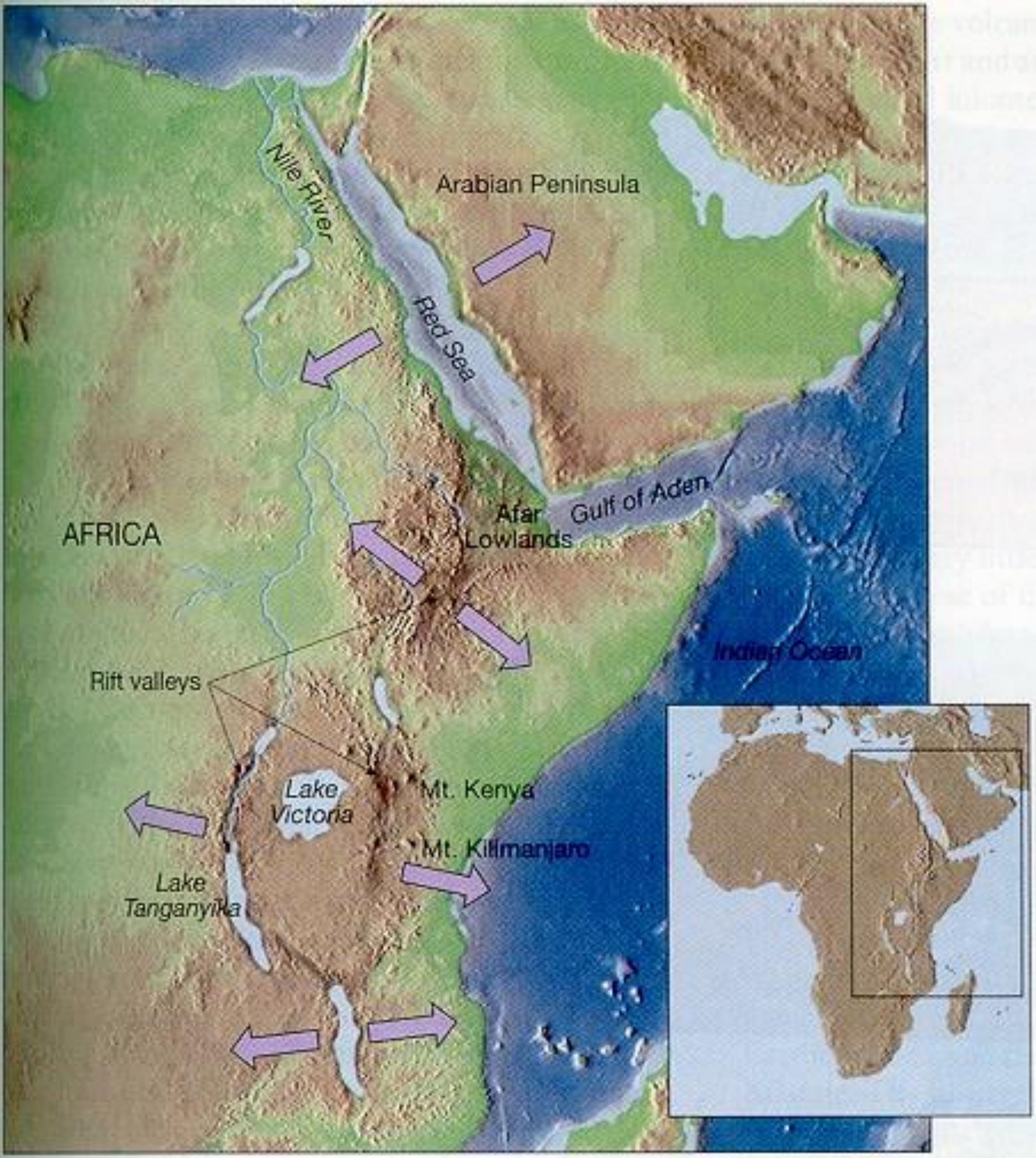

Figure 19.21 East African rift valleys and associated features.

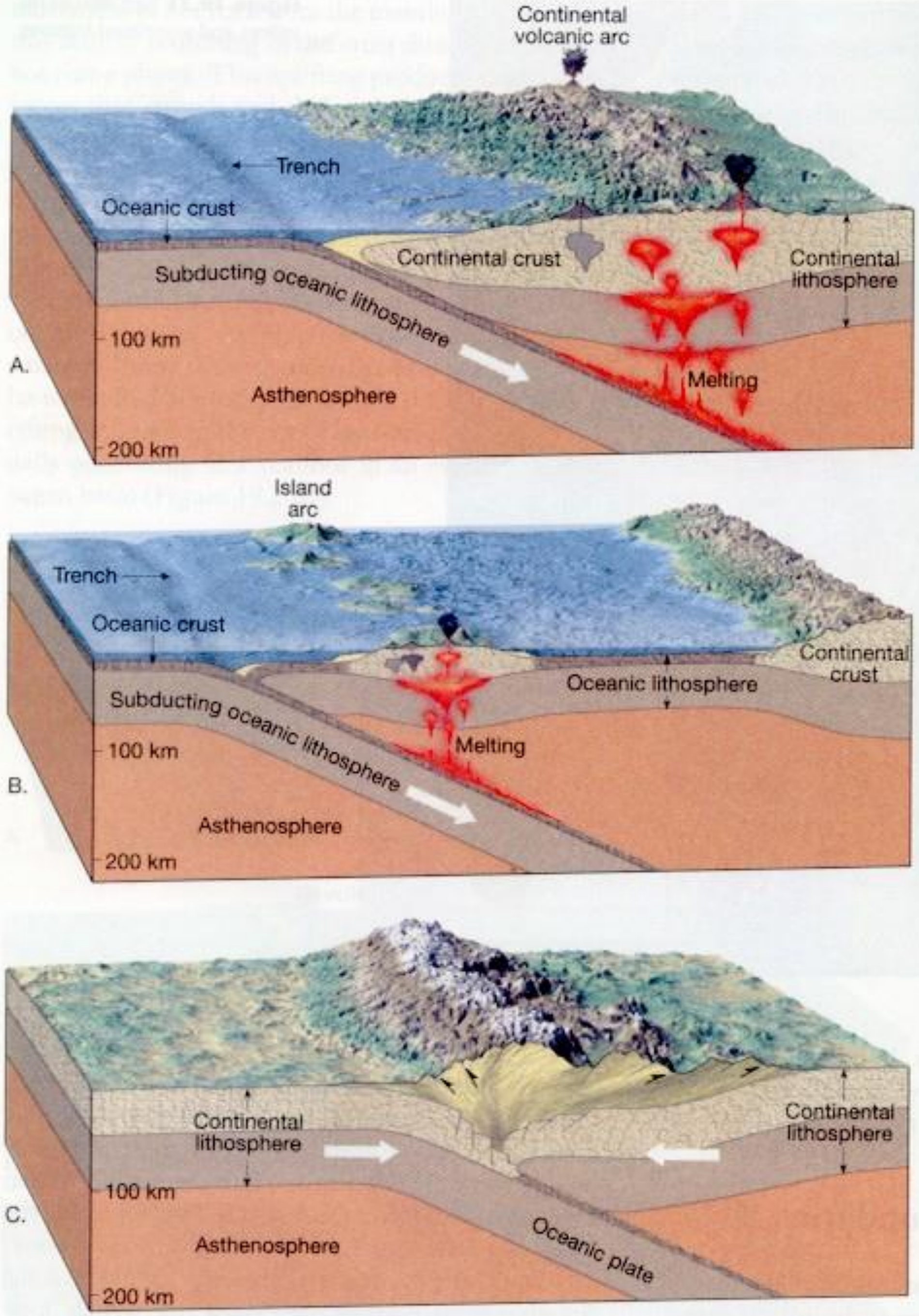

Figure 19.22 Zones of plate convergence.
A. Oceanic–continental.
B. Oceanic–oceanic.
C. Continental–continental.

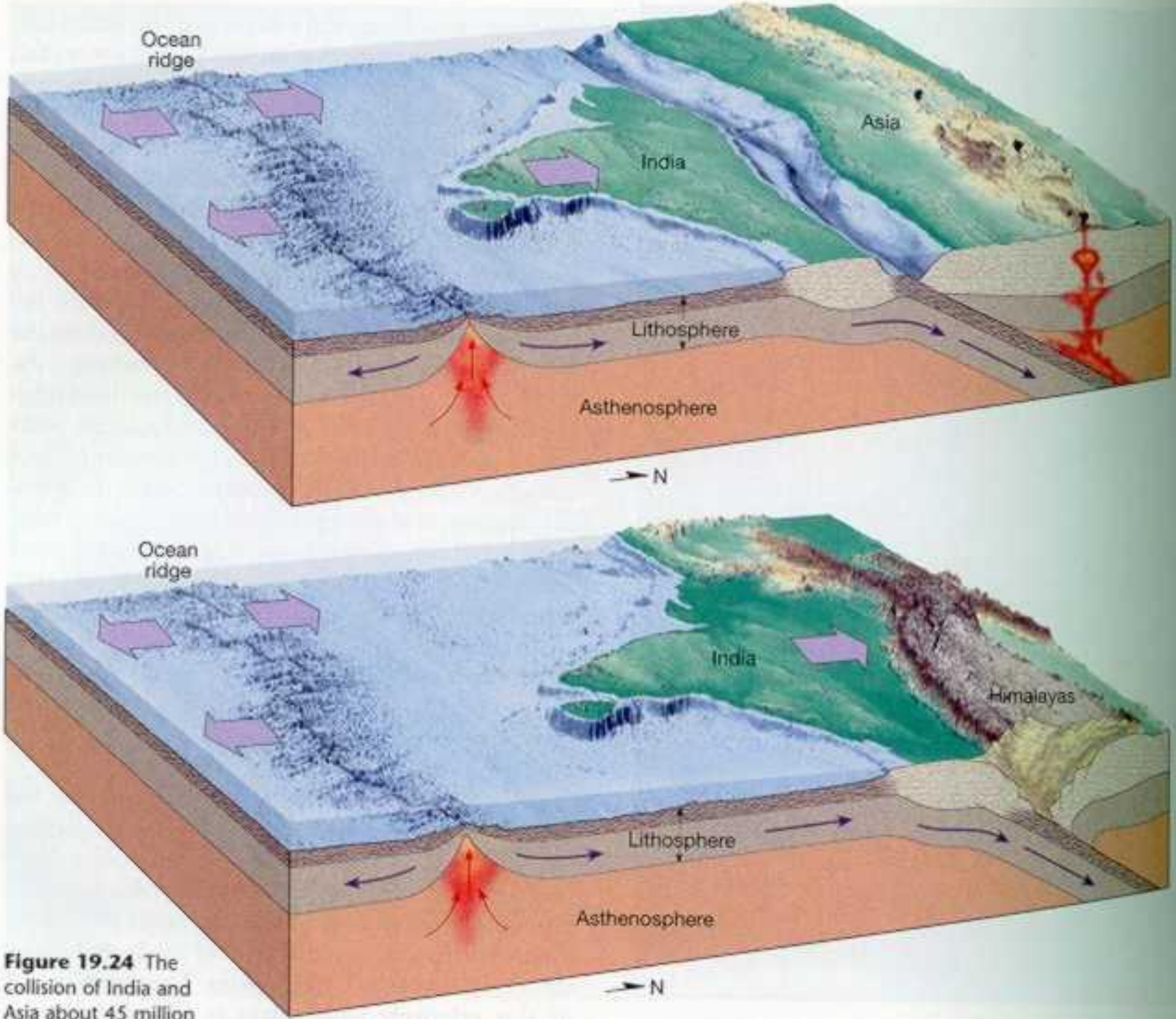

Figure 19.24 The collision of India and Asia about 45 million years ago produced the majestic Himalayas.

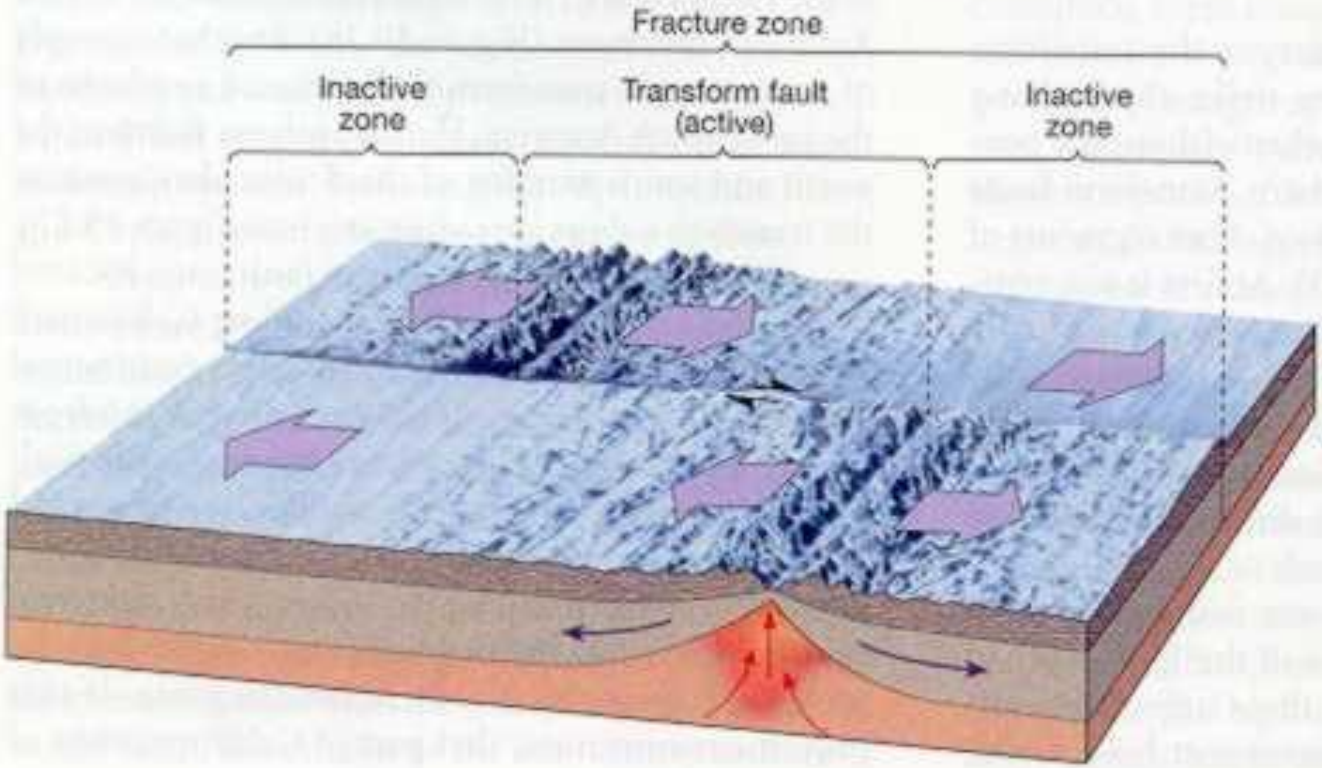

Figure 19.25 Diagram illustrating a transform fault boundary offsetting segments of a divergent boundary (oceanic ridge).

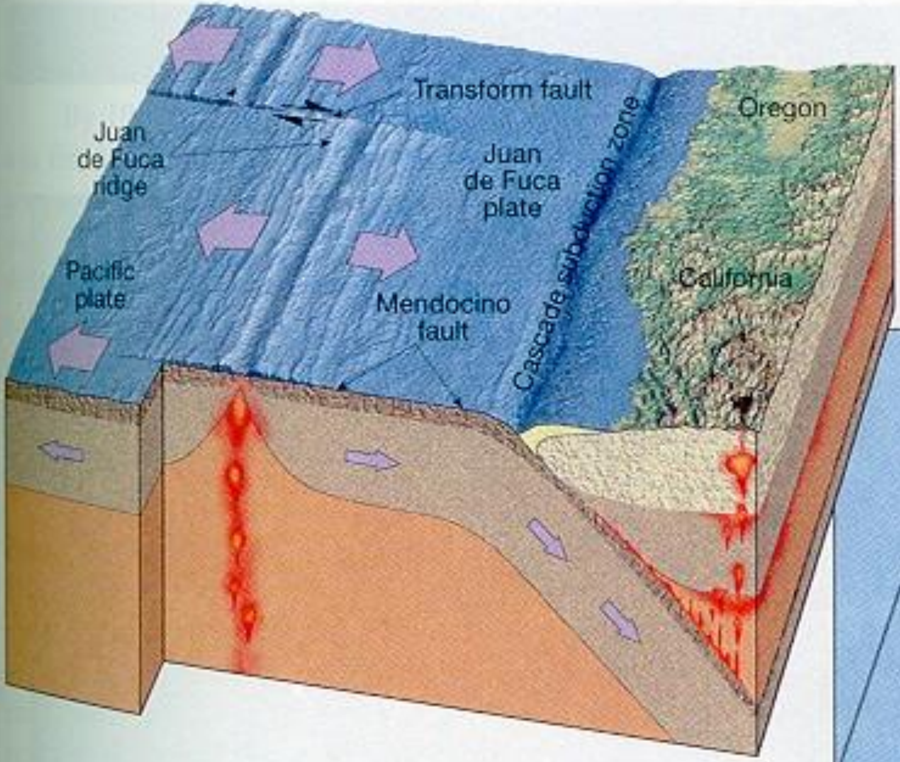

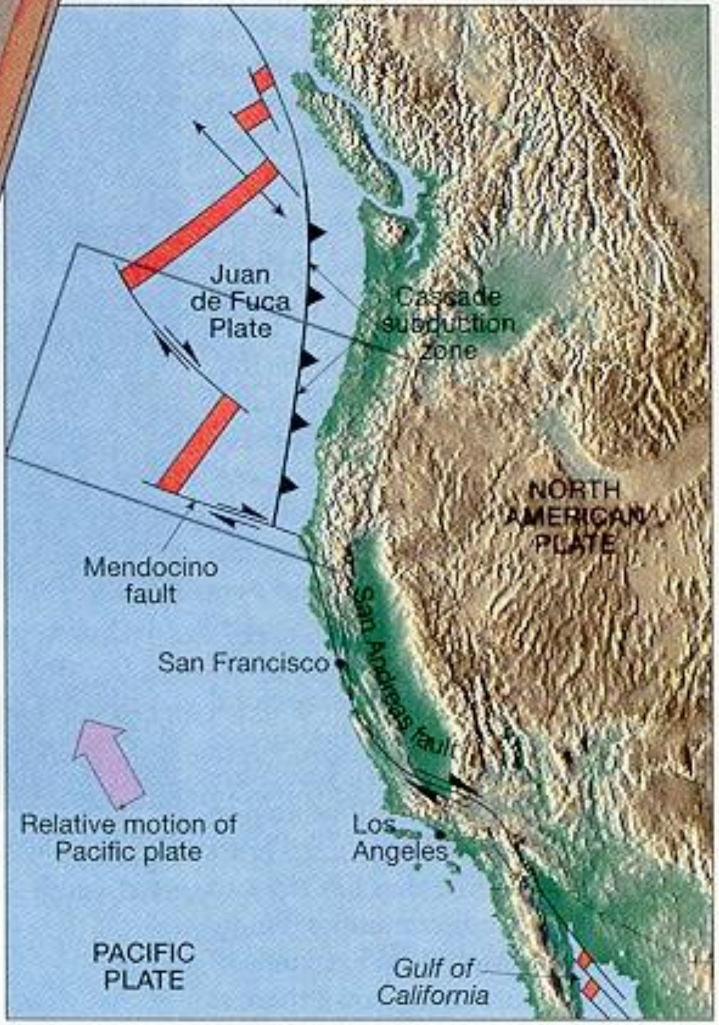

Figure 19.26 The Mendocino transform fault permits the movement of seafloor generated at the Juan de Fuca ridge to move southeastward past the Pacific plate and beneath the North American plate. Thus, this transform fault connects a divergent boundary to a subduction zone. Furthermore, the San Andreas fault, also a transform fault, connects two spreading centers; the Juan de Fuca ridge and a divergent zone located in the Gulf of California.

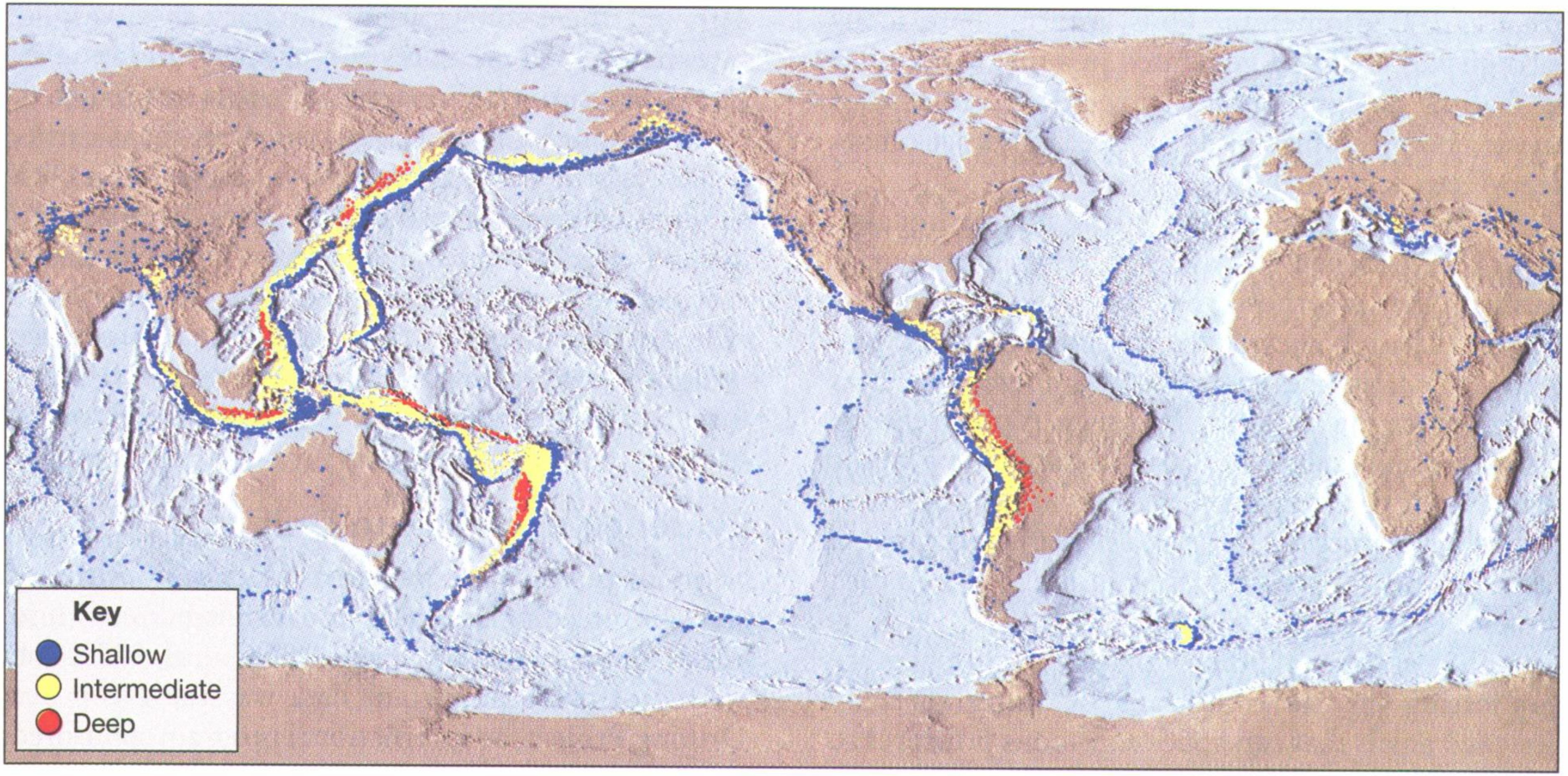

Figure 19.27 Distribution of shallow-, intermediate-, and deep-focus earthquakes. Note that deep-focus earthquakes only occur in association with convergent plate boundaries and subduction zones. (Data from NOAA)

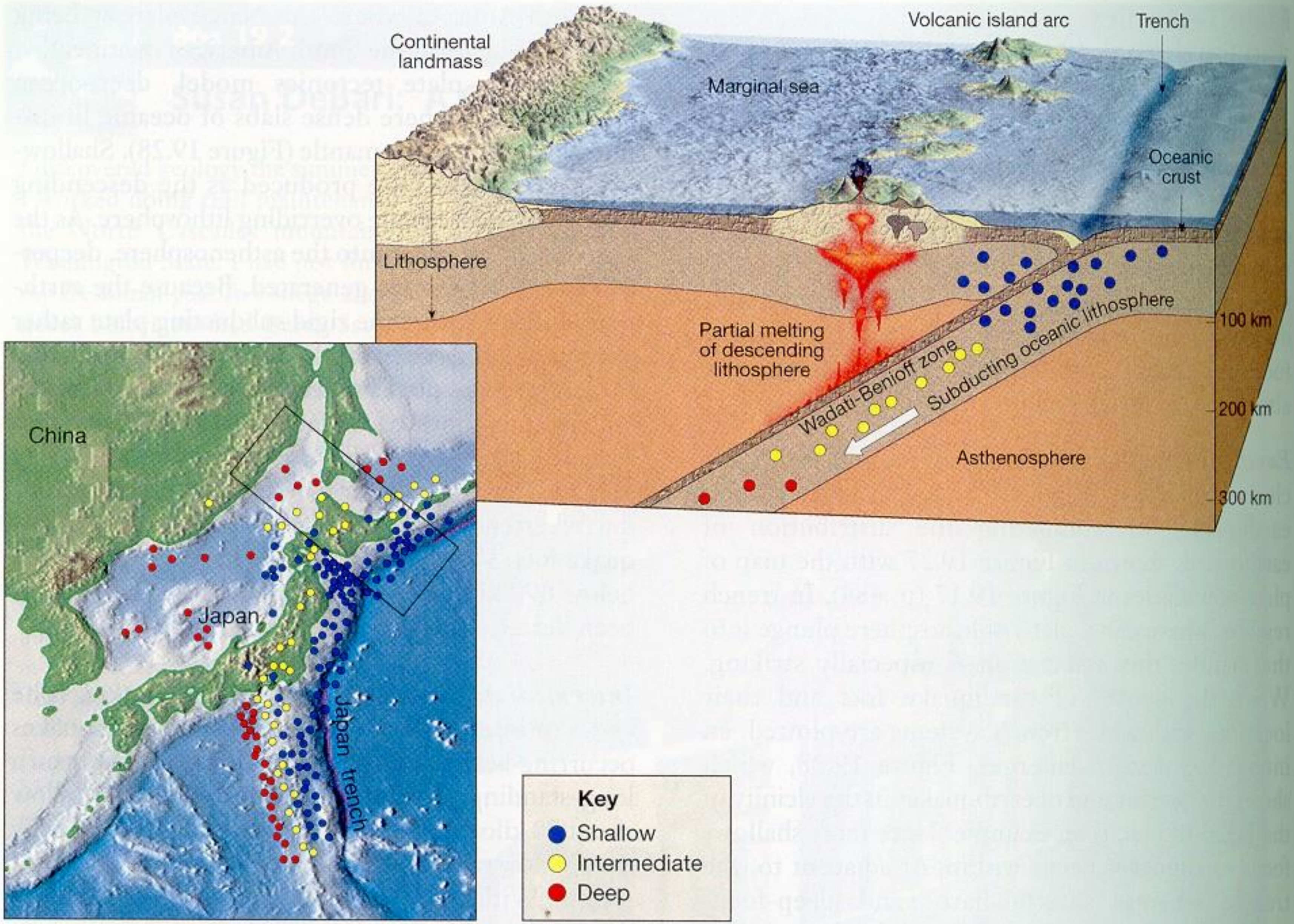

Figure 19.28 Distribution of earthquake foci in the vicinity of the Japan trench. Note that intermediate- and deep-focus earthquakes occur only within the sinking slab of oceanic lithosphere. (Data from NOAA)

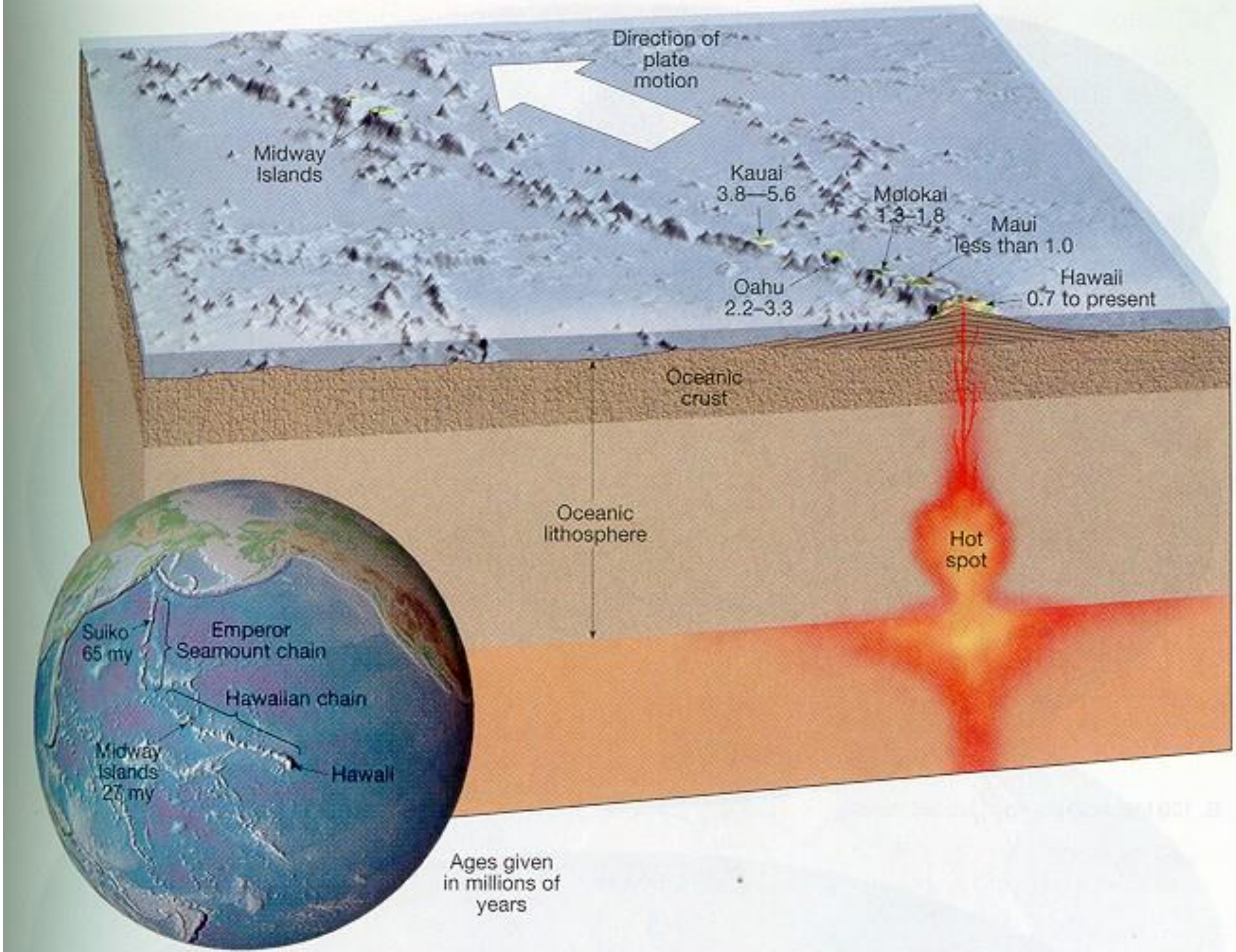

Figure 19.30 The chain of islands and seamounts that extends from Hawaii to the Aleutian trench results from the movement of the Pacific plate over an apparently stationary hot spot. Radiometric dating of the Hawaiian Islands shows that the volcanic activity decreases in age toward the island of Hawaii.

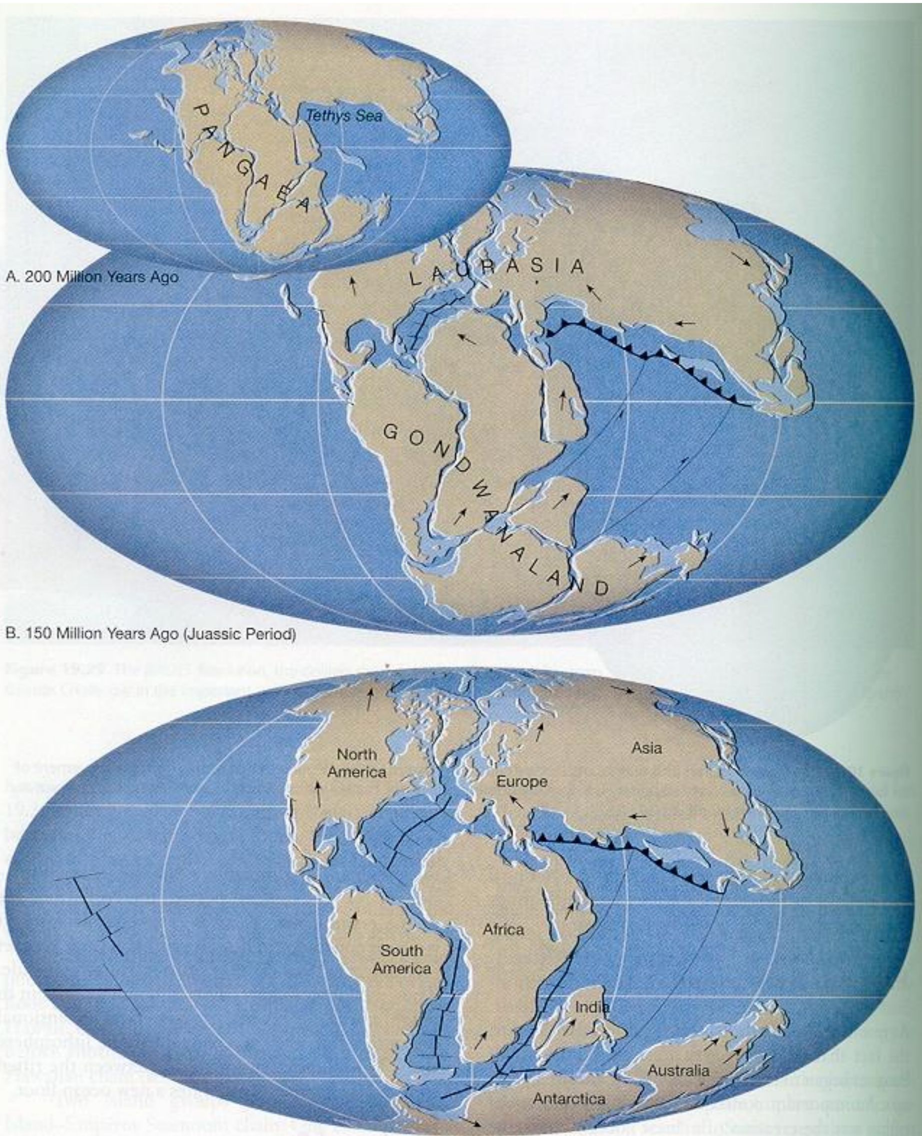

A. 200 Million Years Ago

B. 150 Million Years Ago (Juassic Period)

C. 100 Million Years Ago (Cretaceous Period)

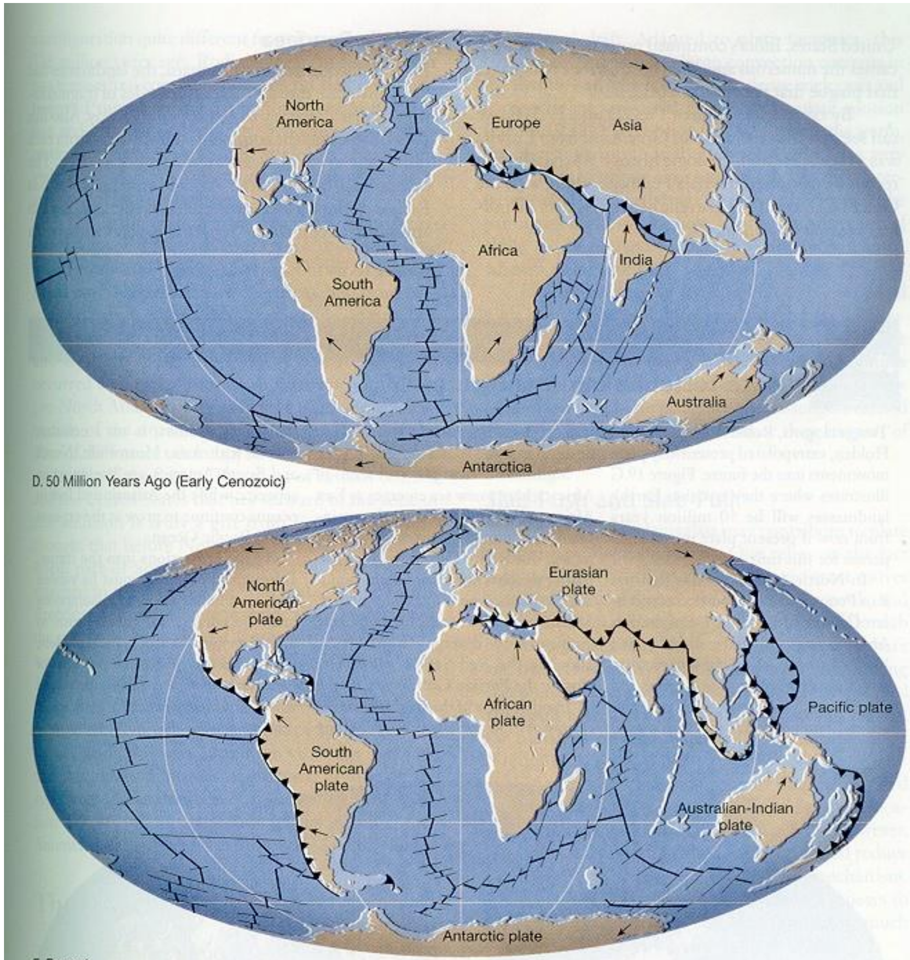

D. 50 Million Years Ago (Early Cenozoic)

E. Present

Figure 19.31 Several views of the breakup of Pangaea over a period of 200 million years.

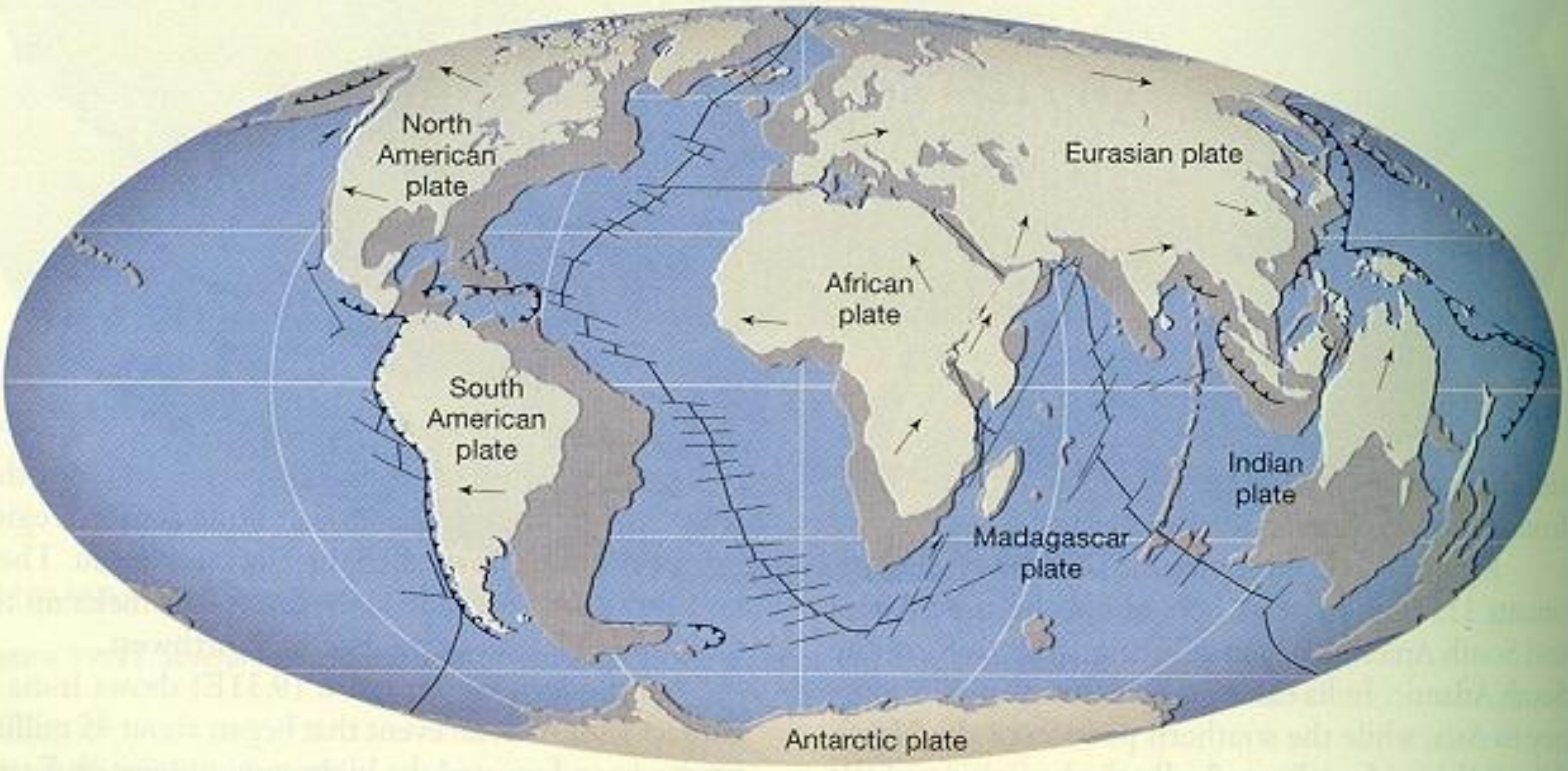

Figure 19.C The world as it may look 50 million years from now. (From "The Breakup of Pangaea," Robert S. Dietz and John C. Holden. Copyright 1970 by Scientific American, Inc. All rights reserved.)

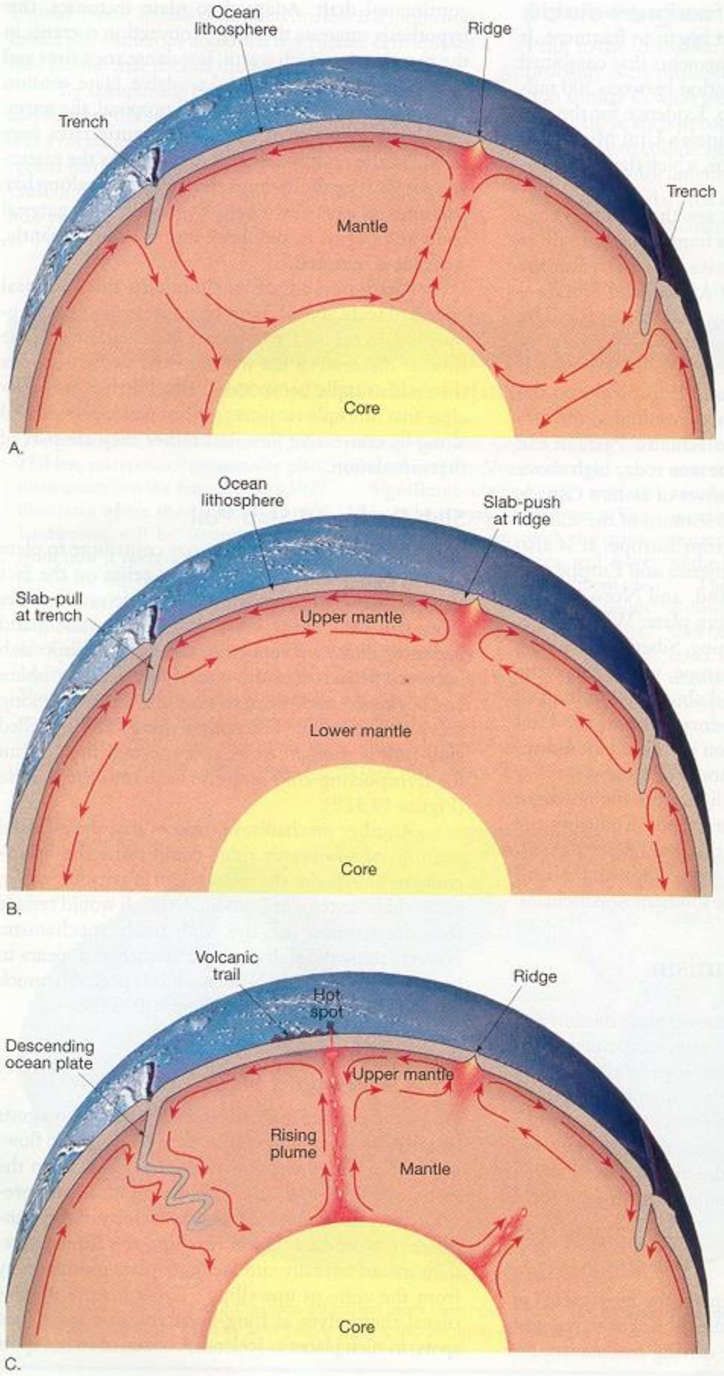

Figure 19.32 Proposed models of the driving force for plate tectonics. **A.** Large convection cells in the mantle may carry the lithosphere in a conveyor-belt fashion. **B.** Slab-pull results because the subducting slab is more dense than the underlying material. Slab-push is a form of gravity sliding caused by the elevated position of lithosphere at a ridge crest. **C.** The hot plume model suggests that all upward convection is confined to a few narrow plumes, while the downward limbs of these convection cells are the cold, dense subducting oceanic plates.